Chemical Engineering Journal 181–182 (2012) 360–370

Contents lists available at SciVerse ScienceDirect

Chemical Engineering Journal

journal homepage: www.elsevier.com/locate/cej

Affecting factors, equilibrium, kinetics and thermodynamics of bromide removal from aqueous solutions by MIEX resin

Lei Ding[a,b,c], Huiping Deng[a,*], Chao Wu[b], Xu Han[a]

[a] Key Laboratory of Yangtze River Water Environment, Ministry of Education, Tongji University, 1239 Siping Road, Shanghai 200092, PR China
[b] School of Civil Engineering and Architecture, Anhui University of Technology, 59 Hudong Road, Maanshan 243002, PR China
[c] Engineering Research Center of Biomembrane Water Purification and Utilization Technology Ministry of Education, Anhui University of Technology, 59 Hudong Road, Maanshan 243002, PR China

ARTICLE INFO

Article history:
Received 22 August 2011
Received in revised form
24 November 2011
Accepted 28 November 2011

Keywords:
Bromide
MIEX resin
Adsorption
Isotherm
Kinetics
Thermodynamics

ABSTRACT

It is necessary to remove bromide from raw water owing to the fact that bromide directly leads to the brominated disinfection byproducts during the disinfection process for drinking water. The adsorption characteristics of bromide by MIEX resin are investigated in a batch mode. Some factors such as initial bromide concentration, contact time, adsorbent dosage, pH of solution and coexistent anions, have significant effect on bromide removal. Five isotherm models, namely, Langmuir, Freundlich, Temkin, Dubinin–Radushkevich and Redlich–Peterson, are used to fit the equilibrium data of bromide on MIEX resin at 303 K. The results show that the adsorption equilibrium can be well fitted by the Freundlich and Redlich–Peterson isotherm models. The pseudo first-order and second-order kinetics models are used to fit the kinetics process of bromide adsorption on MIEX resin. The results demonstrate the adsorption kinetics agree with the pseudo second-order model, indicating the adsorption of bromide on MIEX is chemical sorption. The intra-particle diffusion model is used to further analyze the diffusion mechanism of bromide during the adsorption process. The results imply that the intra-particle diffusion is not the only rate limiting step. The negative ΔG° values indicate that the adsorption of bromide on MIEX resin is thermodynamically feasible and is a spontaneous process. The negative ΔH° and ΔS° show that the adsorption is an exothermic process in nature and the randomness degree at the solid/liquid interface decreases after adsorption.

1. Introduction

Bromide is naturally present in surface and ground water sources due to seawater intrusion, industrial and agricultural wastewater discharge and special geological circumstance [1]. A nationwide survey in China showed that the bromide concentration in water resources was 0.01–6.0 mg L^{-1}, especially up to 6.0 mg L^{-1} in the ground water sources of coastal areas such as Liaoning and Shandong provinces, and even, much higher bromide concentration in the case of sudden polluted surface water sources [2]. Although the bromide itself is not regulated in drinking water standard, the presence of bromide in water sources potentially endangers the security of drinking water supplies due to the occurrence of brominated disinfection byproducts [3]. During the process of chlorination, bromide can be oxidized to HOBr which can react with natural organic matter in water to form brominated organic disinfection byproducts [4]. And the brominated organic disinfection byproducts are more harmful to human health than conventional chlorinated organic disinfection byproducts, which pose even more significant public health risks [5,6]. On the other hand, ozone and/or hydroxyl radical, as promising disinfectants and oxidants, can oxidize bromide in water to hypobromite ion which is then further oxidized to bromate [7–9]. Even, the bromide in water can be also oxidized to bromate during the process of chlorination for drinking water [10,11]. Bromate, as a brominated inorganic disinfection byproduct, has been designated as a Group 2B substance by the International Agency for Research on Cancer due to potential carcinogenic and mutagenic to human organisms [12–14]. So the presence of bromide in raw water is the direct reason leading to the brominated disinfection byproducts. However, the conventional treatment process for drinking water, such as flocculation, sedimentation, filtration and disinfection, is little effective to remove bromide. Thus, removing bromide (the precursor of disinfection byproduct) from raw water, is the most effective and thorough method to solve the brominated disinfection byproducts.

Several attempts have been made for bromide removal [15]. The bromide can be effectively removed by Ag-doped carbon aerogels, but the preparation of Ag-doped carbon aero gels consumes

---

[*] Corresponding author at: Room 215, Mingjing Building, Key Laboratory of Yangtze River Water Environment, Ministry of Education, Tongji University, 1239 Siping Road, Shanghai 200092, PR China. Tel.: +86 13311875226.
E-mail address: denghuiping@sina.com (H. Deng).

1385-8947/$ – see front matter © 2011 Elsevier B.V. All rights reserved.
doi:10.1016/j.cej.2011.11.096

expensive metal ion and the carbon aero-gels possibly leach [16,17]. The enhanced coagulation by aluminum chloride can remove the bromide of 62.1–87.0% in raw water, but the bromide may seep into groundwater when the sludge containing bromide is disposed by landfill [18,19]. Also, the calcined layered double hydroxides can remove the bromide in drinking water, but when the saturated adsorbents are regenerated, plenty of alkaline waste is discharged [20]. Electrochemical oxidation is an excellent approach to remove lower bromide by oxidation of bromide to bromine and the volatilization of bromine, but different type of brominated disinfection products may be produced in this process [15,21]. Membrane filtration, such as nanofiltration, ultra filtration and reverse osmosis, is used to reduce bromide, but is not a cost-effective method because of expensive membrane [22]. Boyer and Singer found the magnetic ion exchange (MIEX) resin could remove bromide from raw water to a certain extent [23], as well as dissolved organic compounds. Bromide removal by MIEX resin is focused on in this study.

The magnetic ion exchange (MIEX) resin is a strong-base resin with a macro-porous, polyacrylic matrix, and is typically used with chloride as the exchangeable ion [24]. The iron oxide integrated into the matrix of resin facilitates the aggregation and settling of MIEX after adsorbing pollutants. Extensive research has shown that it is an effective technology to remove dissolved organic matters from raw water and wastewater by MIEX [25–30]. And the hybrid processes of MIEX and coagulation, activated carbon adsorption, chlorine, membrane filtration, can be used to remove diversely organic pollutants, reduce membrane fouling and decrease operating pressure on both sides of membrane [31–35]. The MIEX was designed specifically to remove dissolved organic matters from raw drinking waters, but, as an anion exchange resin, it can be used to remove inorganic anions such as bromide. This has been verified by some researchers [24,36]. However, the present studies mainly focused on low concentration bromide in surface water resources. Also, the factors affecting efficacy of bromide removal, such as solution pH, temperature, agitation speed, MIEX dosage, anions, have not been elucidated systematically and thoroughly yet, which are crucial to optimize the operating parameters of bromide removal process by MIEX. In addition, the equilibrium, kinetics and thermodynamics process of bromide adsorption on MIEX have not been reported yet, which are essential to interpret the mechanism of bromide removal by MIEX and further enhance and improve the properties of MIEX itself.

Accordingly, the goal of this work is to systematically evaluate the removal characteristics of high concentration bromide by MIEX, with a view to providing a theoretical basis for bromide removal from ground water or sudden polluted surface water. The specific objects of this study are to (1) investigate the effects of different factors such as MIEX dosage, bromide concentration, contact time, solution pH, temperature, agitation intensity and other anions, on bromide removal; (2) simulate the equilibrium adsorption data with different isotherm models such as Langmuir, Freundlich, Temkin, Dubinin–Radushkevich and Redlich–Peterson, and identify the equilibrium adsorption model of bromide on MIEX; (3) analyze the kinetics data and interpret the kinetics process of bromide adsorption on MIEX resin; (4) calculate the thermodynamics parameters such as ΔG°, ΔH°, ΔS° and elucidate the thermodynamic process of bromide adsorption on MIEX.

2. Materials and methods

2.1. Materials

2.1.1. Adsorbent

The MIEX resin, used as adsorbent in this study, is obtained from the China Agent of Orica Watercare of Victoria. The virgin MIEX resin is stored in water. And the average diameter of MIEX resin particles is 180 μm. The MIEX resin is washed repeatedly with ultra-pure water to remove the impurities before used and then is stored in ultra-pure water. A certain volume of resin used in adsorption experiment is taken with a 5 mL glass centrifuge tube whose accuracy is 0.1 mL. Taking 1.0 mL MIEX resin as an example illustrates the process of taking a certain volume of resin. First, approximately transfer 1.2 mL MIEX resin to centrifuge tube. Then add ultra-pure water to the scale mark of 5 mL, and take the resin particles still setting for 30 min. Finally, take out the excess resin and ultra-pure water above the scale mark of 1.0 mL from the centrifuge tube and the 1.0 mL MIEX resin remaining in centrifuge tube is obtained.

2.1.2. Chemicals and adsorbate

All chemicals used in this study are guaranteed reagent grade or better and purchased from Sinopharm Chemical Reagent Co., Ltd., China. The standard stock solutions and samples for a calibration curve are prepared by ultra-pure water obtained from Millipore Super-Q plus water system.

Potassium bromide (KBr) is used as an adsorbate in this study. A standard stock solution of bromide ion (Br^-) is prepared by dissolving accurately weighed sample of Potassium bromide in ultra-pure water to give a concentration of 1000 mg L^{-1}. The test solutions of bromide ion of various concentrations are obtained by diluting the standard stock solution with distilled water when necessary.

2.2. Methods

2.2.1. Kinetic studies

The kinetic studies are conducted by the batch mode. Fixed dosage (0.5 mL) of MIEX resin is added into a set of 1000 mL beakers containing 500 mL adsorbate with the concentration of 5 mg L^{-1}, respectively. Then the beakers are sealed with aluminum foil and kept on the digital display stable temperature magnetic stirrer (78HW-1). The slurries are mixed with a constant agitation speed of 100 rpm at 288 K. The aqueous samples are taken out at preset time intervals and the solid adsorbent is separated from the mixture by using a 0.45 μm Millipore membrane filter. The bromide ion remaining in filtrate is determined. In order to compare the kinetics process with initial bromide concentration of 5 mg L^{-1}, the similar kinetic experiments are carried out by varying bromide concentration (10, 20 mg L^{-1}). In these experiments, the pH of the bromide solution is kept originally without any adjustment. All the experiments are carried out in triplicate and the average values are reported herein.

The bromide uptake on MIEX at time t, q_t (mg mL^{-1}), is calculated by Eq. (1):

$$q_t = \frac{(C_0 - C_t)V}{W} \qquad (1)$$

where C_0 and C_t (mg L^{-1}) are the liquid-phase concentrations of bromide at initial and at time t, respectively. V (L) is the volume of solution and W (mL) represents the volume of adsorbent.

2.2.2. Independent variable studies

The procedure of independent variable experiments is similar to that of kinetic studies. However, the slurries are mixed continuously for 90 min. Thereafter, the bromide in filtrate is analyzed. Effects of different parameters on bromide removal are employed by varying MIEX dosage, agitation speed, initial pH of solution and temperature. When investigating the impact of one variable on bromide removal, only this variable is changed, while other variables remain unchanged. The initial pH values of bromide solutions are adjusted by adding 0.1 M HCl or 0.1 M NaOH solutions when necessary. All the experiments are carried out in triplicate and the average values are reported herein. After 90 min adsorption, the uptake of bromide on MIEX resin is calculated by Eq. (1) and the removal rate (E) of bromide is calculated by bromide concentration change in solution before and after adsorption.

2.2.3. Adsorption equilibrium studies

Batch equilibrium adsorption tests of bromide on MIEX are conducted at 303 K. Fixed dosage (0.5 mL) of MIEX resin is added into a set of 1000 mL beakers containing 500 mL adsorbate with various initial bromide concentrations (1–10 mg L^{-1}), respectively. Then the suspensions are mixed on the digital display stable temperature magnetic stirrer with a constant agitation speed of 100 rpm for 2 h. The similar operation to the kinetic experiments is applied to separate the solid adsorbent from the suspension. And the bromide in filtrate is determined. The equilibrium adsorption capacity is calculated by Eq. (2):

$$q_e = \frac{(C_0 - C_e)V}{W} \tag{2}$$

where q_e (mg mL^{-1}) and C_e (mg L^{-1}) are the bromide amount adsorbed by MIEX and bromide concentration in aqueous solution when equilibrium is achieved, respectively.

2.2.4. Analysis methods and instruments

The pH of solution is measured using a pH meter (pHS-3C model, Leici, China). Prior to each use, the pH meter is calibrated. Bromide is determined using suppressed conductivity detection on a Shimadu Ion Chromatograph (Shimadu, Japan) with an IC SI-52G guard column (4.6 mm × 10 mm, Shodex, Japan) and an IC SI-52 4E analytical column (4.0 mm × 250 mm, Shodex, Japan) according to the standard method [37]. The 3.6 mM sodium carbonate (Na_2CO_3) is used as solvent and the flow rate of the solvent is 0.8 mL min^{-1} with a sample injection volume of 20 μL. The temperature of the column and detector compartment is set to 45 °C. The correlation coefficient of calibration curve (R^2) is 0.9999. Each sample is analyzed in duplicate and averaged. The precision is checked by calculating the percent difference within 15% between duplicate samples.

3. Results and discussion

3.1. Effect of contact time and initial bromide concentration

The effects of contact time and various initial bromide concentrations on bromide removal are shown in Fig. 1. The similar trend of bromide removal can be seen in Fig. 1a when the bromide concentration varies from 5 to 20 mg L^{-1}. Each plot of q_t versus contact time can be divided into three stages. The uptake of bromide on MIEX dramatically increases with an increase in contact time within initial 30 min (the first stage). Thereafter, the uptake slowly increases as time elapses from 30 to 60 min (the second stage). Finally (the third stage), there is no significant change in uptake after 60 min, which means that the adsorption of bromide on MIEX resin reaches equilibrium. In initial stage, for the virgin MIEX resin, the accessible adsorption sites are vacant, leading to the uptake of bromide on MIEX resin increasing sharply. Also, the greater concentration gradient between the bromide solution and the surface of MIEX resin accelerates the diffusion process of bromide from the liquid-phase to solid, causing the fast increase of uptake in initial stage [38]. As the adsorption continues (the second stage), the reduction of available adsorption sites, the slower diffusion because of the smaller concentration gradient and the repulsive forces of bromide ions between adsorbed on MIEX resin and in solution, result in the decrease in adsorption rate. After 60 min (the third stage), the uptake maintains constant approximately because the adsorption equilibrium is reached.

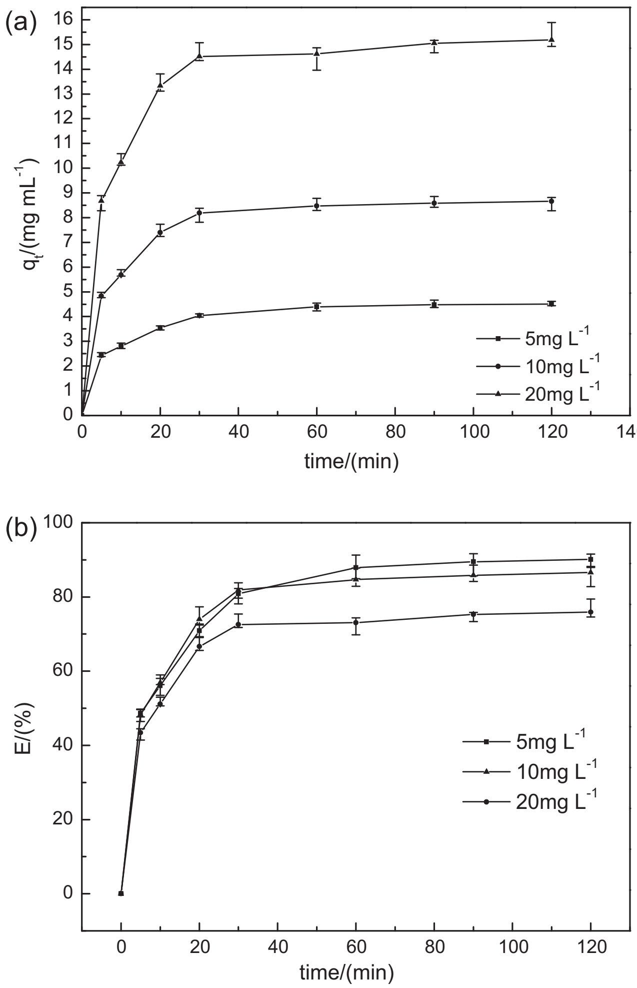

Fig. 1. Effect of initial bromide concentration and contact time on bromide removal (adsorbent dosage = 1.0 mL L^{-1}; agitation speed = 100 rpm; pH without any adjustment; temperature = 285 K).

Also, it is clear from Fig. 1a that there are apparent differences in the uptake of bromide on MIEX resin for various initial bromide concentrations, and the uptake increases with increasing the initial bromide concentration from 5 to 20 mg L^{-1}. For example, after 60 min adsorption, the amounts of bromide adsorbed are 4.40, 8.47 and 14.62 mg mL^{-1} for various initial bromide concentrations of 5, 10 and 20 mg L^{-1}, respectively. This phenomenon may be interpreted by the following facts: (1) the probabilities of interaction between the adsorption sites and bromide are greater for higher initial bromide, which is crucial to adsorption occurrence; (2) the greater concentration gradient in a high bromide concentration solution makes the bromide adsorbed on surfaces of MIEX into the pores, which may give some available sites to adsorb other bromide again [39].

In addition, it is observed from Fig. 1b that the removal rates of bromide are close approximately for 5 and 10 mg L^{-1} bromide concentrations, but the removal rates of bromide for 20 mg L^{-1} bromide concentration are much smaller than those for 5 and 10 mg L^{-1} bromide concentrations. This is attributed to the fact that the available adsorption sites are the fixed amounts for 0.5 mL of MIEX resin and the adsorption sites are sufficient to remove lower concentration bromide (<10 mg L^{-1}), conversely, under the experimental conditions the inadequate adsorption sites for the higher concentration bromide (>20 mg L^{-1}) cause the decline of bromide removal rate although MIEX resin has a theoretical exchange capacity of 0.5 meq L^{-1}.

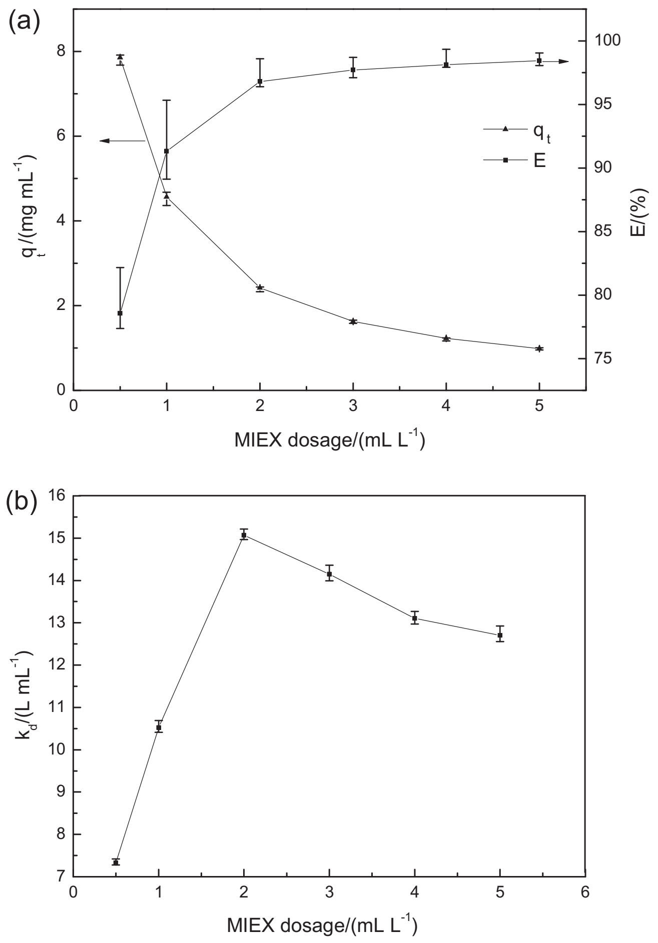

Fig. 2. Effect of adsorbent dosage on bromide removal (bromide concentration = 5 mL L^{-1}; agitation speed = 100 rpm; pH without any adjustment; temperature = 285 K).

3.2. *Effect of adsorbent dosage*

The effects of different MIEX dosage on bromide removal are evaluated by varying the dosage from 0.5 to 5 mL L^{-1} and the results are presented in Fig. 2. The removal rate of bromide increases from 78.56% to 98.45% when the dosage of MIEX resin is increased from 0.5 to 5 mL L^{-1}. This is attributed to the increased total available adsorption sites. Further, the removal rate of bromide rapidly increases from 78.56% to 91.32% with increasing dosage from 0.5 to 1.0 mL L^{-1}, however, only increases from 91.32% to 98.45% with increasing dosage from 1.0 mL L^{-1} to 5.0 mL L^{-1}. MIEX resin has a theoretical capacity of 0.5 meq mL^{-1} resin. Generally the working exchange capacity is much smaller than the theoretical capacity due to different working conditions. For bromide of 500 mL with the concentration of 5 mg L^{-1}, the accessible adsorption sites are insufficient to remove bromide when the dosage used is below 1 mL L^{-1}. Thus, the dosage becomes the limiting factor of bromide removal, which induces the sharply increase in bromide removal with increasing dosage. Nevertheless, for the high MIEX dosage (>1.0 mL L^{-1}), the adsorption sites are adequate and not utilized effectively. This leads to the low increase in bromide removal with increasing resin dosage from 1.0 mL L^{-1} to 5.0 mL L^{-1}.

Fig. 2a also reflects that the amount of bromide adsorbed on MIEX resin decreases from 7.86 to 0.98 mg mL^{-1} with an increase in MIEX dosage from 0.5 to 5.0 mL L^{-1}. The decrease of the amount of bromide adsorbed on MIEX resin may be caused by the lower utilization of the adsorbents adsorptive capacity. Also, the heterogeneous surface adsorption sites of MIEX resin may result in the decrease in amount of bromide adsorbed on MIEX resin. According to the surface site heterogeneity model, the surface is composed of sites with a spectrum of binding energies, and at low adsorbent dose, all types of sites are entirely exposed and the adsorption on the surface is saturated faster, showing a higher q_t value. But at higher adsorbent dose, the availability of higher energy sites decreases with a larger fraction of lower energy sites occupied, resulting in a lower q_t value [40]. In addition, the aggregation/agglomeration of adsorbent particles at higher dosage may lead to a decrease in the surface area and an increase in the path length of diffusion, which decreases the amount of bromide adsorbed on MIEX resin probably [41].

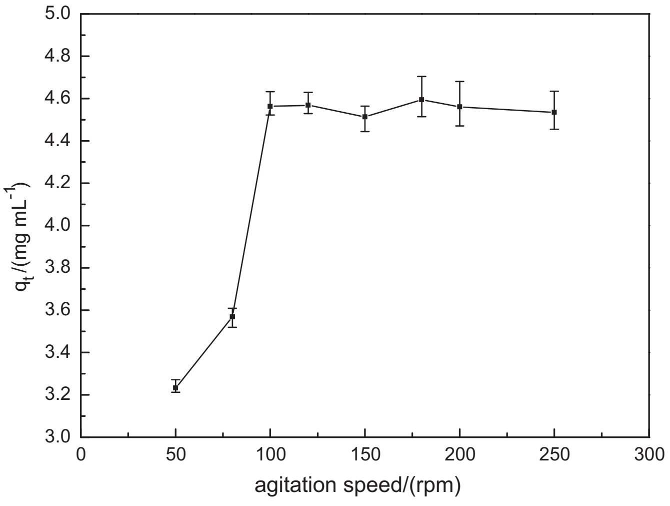

Fig. 3. Effect of agitation speed on bromide removal (bromide concentration = 5 mL L^{-1}; adsorbent dosage = 1.0 mL L^{-1}; pH without any adjustment; temperature = 285 K).

The solid–liquid distribution coefficient (K_D) of bromide on MIEX resin and in solution after adsorption can be calculated by the Eq. (3):

$$K_D = \frac{(C_0 - C_t)}{C_t} \times \frac{V}{W} \tag{3}$$

The distribution coefficient, K_D, increases from 7.33 to 15.07 L mL^{-1} with an increase in dosage from 0.5 to 2.0 mL L^{-1}, while declines from 15.07 to 12.70 L mL^{-1} with increasing the dosage from 2.0 to 5.0 mL L^{-1} (observed from Fig. 2b). The change law of K_D may be caused by the fact that the adsorptive sites are used effectively for the dosage of 0.5–2.0 mL L^{-1}, whereas are not for the dosage of 2.0–5.0 mL L^{-1}. The similar research results were reported in the process of bromide removal by MgAl–CO_3 layered double hydroxides [20]. Therefore, the dosage of 1.0 mL L^{-1} is selected for the following experiments.

3.3. *Effect of agitation speed*

The effects of agitation speed on bromide removal are conducted by varying the agitation speed from 50 to 250 rpm, and the results are shown in Fig. 3. The amount of bromide adsorbed on MIEX resin increases from 3.23 to 4.56 mg mL^{-1} with increasing the agitation speed from 50 to 100 rpm. For the lower agitation speed (for example 50 rpm), the MIEX resin particles are not mixed completely with the bromide solution and it is observed that some particles aggregate and settle to the bottom of breaker in the experimental process. So the interaction between the bromide and adsorption sites is not sufficient and the available sites are not used fully, resulting in the lower uptake of bromide. The MIEX resin particles are dispersed

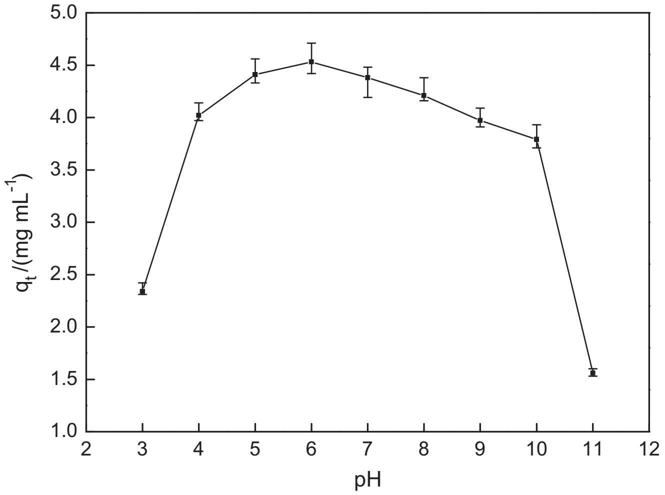

Fig. 4. Effect of pH of solution on bromide removal (bromide concentration = 5 mg L^{-1}; adsorbent dosage = 1.0 mL L^{-1}; agitation speed = 100 rpm; temperature = 285 K).

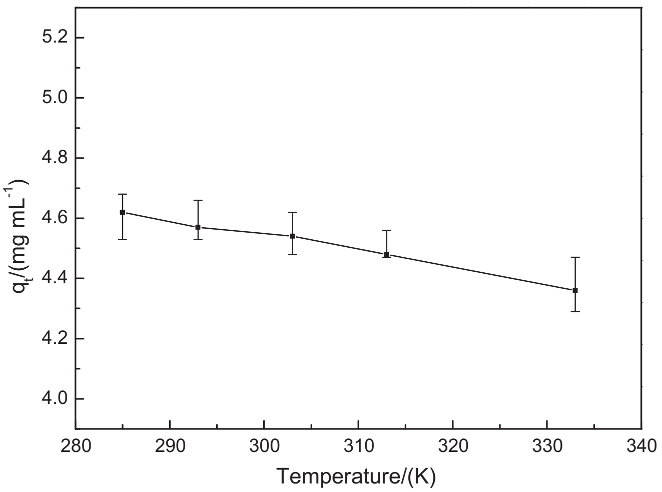

Fig. 5. Effect of temperature of solution on bromide removal (bromide concentration=5 mg L^{-1}; adsorbent dosage = 1.0 mL L^{-1}; agitation speed = 100 rpm; pH without any adjustment).

evenly in the bromide solution with increasing the agitation speed to 100 rpm, causing the increase in uptake. Whereas no considerable increase in uptake is observed with further increasing agitation speed from 100 to 250 rpm. This may be because that after being mixed with bromide solution evenly, the accessible adsorption sites of 0.5 mL MIEX are constant. In addition, the external mass transfer becoming negligible may also induce the approximately constant uptake when the agitation speed is above 100 rpm [42]. The agitation speed of 100 rpm is selected in the following experiments.

3.4. *Effect of initial pH of solution*

The pH is an important parameter which affects most of solid/liquid system. The effects of different initial pH of solution on bromide removal are employed by varying the initial pH of solution from 3 to 11, and the results are given in Fig. 4. The uptake of bromide on MIEX increases from 2.34 to 4.53 mg mL^{-1} with the pH being increased from 3 to 6. This may be due to the fact that the chloride ions are introduced into the bromide solution when hydrochloric acid is used to adjust the bromide solution to low pH, and restrain the exchange behavior of bromide ions with chloride ions used as exchange reaction on MIEX resin surface. However, the uptake decreases from 4.53 to 1.56 mg mL^{-1} with increasing the initial pH of solution from 6 to 11. This may be interpreted by the fact that the hydroxyl competitively adsorbs on MIEX resin with bromide. The decrease in pH of solution after adsorption (shown in Table 1) further verifies some hydroxyl ions are adsorbed on MIEX resin. In addition, the results of FTIR (Fourier Translation Infrared spectroscopy) for the MIEX resin used at pH 11.00 show that the hydroxyls have been exchanged on the surface of MIEX resin. The pH of nature water body generally varies in the ranges of 6–9. The percent removal of bromide is above 80% (not shown in Fig. 4) in this study when the initial pH of bromide solution ranges from 4 to 9, indicating it is appropriate that the MIEX resin can be used to remove bromide in nature water body.

3.5. *Effect of temperature of solution*

The temperature of solution plays an important role in the solid–liquid adsorption system. The effects of different temperature of solution are investigated by varying the temperature of solution from 285 to 333 K and the results are shown in Fig. 5. It can be observed that the amount of bromide adsorbed on MIEX resin slightly decreases from 4.62 to 4.36 mg mL^{-1} with increasing temperature of solution from 285 to 333 K. This indicates that the adsorption of bromide on MIEX resin may be exothermic in nature, thus resulting in the decreased uptake with increasing the temperature of solution. Thus elevating temperature of bromide solution is adverse for the adsorption of bromide on MIEX resin. On the other hand, the high temperature (for example, >50 °C) may bring about the decomposition of quaternary amine groups on resin surface, also leading to a decrease in uptake [43]. The percent removal of bromide decreases from 92.4% to 87.2% (not given in Fig. 5) with increasing temperature of solution from 285 to 333 K. The slight decrease in removal rate of bromide shows that the temperature of solution has not obvious effect on bromide removal. So the MIEX resin can be used to remove bromide from raw water not only in summer but also in winter. The similar result of removing anions from aqueous solution by other type resin was reported [44].

3.6. *Effect of coexistent anions*

Various inorganic anions such as chloride, sulfate and carbonate, are often found in nature water body. They may compete for the active adsorption sites due to the different affinities on the MIEX resin surface. Accordingly, it is of great importance to employ the effects of coexistent anions on bromide removal by MIEX resin. The effects of different anions on bromide removal are conducted by varying different type anions (Cl^-, SO_4^{2-} and CO_3^{2-}) with constant concentration (1 meq L^{-1}) and the results are depicted in Fig. 6. The uptake of bromide on MIEX resin is 4.65 mg mL^{-1} when no other anion is added into bromide solution. When chloride, carbonate and sulfate are added into bromide solution, the uptakes of bromide on MIEX resin are 3.50, 2.10, and 1.05 mg mL^{-1}, respectively. This shows that each type anion causes the decrease in the uptake of bromide on MIEX resin to a certain extent. This can be explained by the fact that the competition between each type anion and bromide for the adsorption active sites of MIEX resin surface occurs [45]. But it is also observed from Fig. 6 that the impact of each type anion on bromide removal is different and the following sequence is given: $SO_4^{2-} > CO_3^{2-} > Cl^-$. This is approximately consistent with the affinities between anions and adsorption active sites of strong alkali anion resin. Some research results showed also bromide removal was affected by the chloride, sulfate and water alkalinity [24,46].

Table 1
pH of solution before and after adsorption.

Initial pH	3.02	4.00	5.01	6.00	7.06	8.11	9.05	10.00	11.05
pH after adsorption	3.12	4.36	5.17	6.07	6.64	6.69	7.04	7.25	9.56

3.7. Adsorption isotherm

Adsorption isotherm is a relationship curve that describes the adsorbate distribution between adsorbed on adsorbent and in solution when adsorption equilibrium is reached at a constant temperature. It is significantly important for adsorption system, for it can be used to compare the properties with different adsorbents quantitatively, elucidate the adsorption state of adsorbate on adsorbent surface and calculate adsorption parameters such as theoretical adsorption capacity, adsorption heat. So adsorption isotherm usually provides some insight in sorption mechanism, surface properties and affinity of adsorbent [39].

The results of adsorption equilibrium of bromide on MIEX resin at 303 K are given in Fig. 7. The equilibrium data are fitted by five isotherm models named Langmuir, Freundlich, Dubinin–Radushkevich (D–R), Temkin and Redlich–Peterson (R–P), respectively. These isotherm models can be expressed by Eqs. (4)–(8) [39,47]:

$$\text{Langmuir}: \frac{C_e}{q_e} = \frac{C_e}{q_{\max}} + \frac{1}{q_{\max} b} \tag{4}$$

$$\text{Freundlich}: \log q_e = \frac{\log C_e}{n} + \log k_f \tag{5}$$

$$\text{D–R}: \ln q_e = -B_{DR}\varepsilon^2 + \ln q_{\max} \tag{6}$$

$$\text{Temkin}: q_e = B \ln C_e + B \ln A \tag{7}$$

$$\text{R–P}: \ln\left(K_R \frac{C_e}{q_e} - 1\right) = g \ln C_e + \ln a_R \tag{8}$$

where q_{max} (mg mL^{-1}), is the theoretical maximum bromide uptake, and b is the Langmuir model constant. n and k_f are the Freundlich model constants. B_{DR} and ε are the Dubinin–Radushkevich model constant and the Polanyi potential, respectively.

The validity of isotherm models used in this study is assessed by correlation coefficient (R^2) and standard deviation (SD). For different isotherm models, a high correlation coefficient and a low standard deviation represent a good regression. A correlation coefficient can be obtained from the Origin 8.0 software and a standard deviation can be calculated by the Eq. (9) [48]:

$$\text{SD} = \sqrt{\frac{\sum[(q_{\exp} - q_{cal})/q_{\exp}]^2}{n-1}} \tag{9}$$

where n is the total number of experiment data, and $q_{\exp}$ and q_{cal} are the experimental and calculated values, respectively.

The fitted results of all isotherm models investigated in this study are presented in Table 2, and the predicted curves by five isotherm models mentioned above are also depicted in Fig. 7. Compared with Langmiur, Temkin, and D–R isotherm models which give lower correlation coefficients with the values of 0.9721, 0.9659 and 0.9415 respectively, the highest regression correlation coefficients (0.9946) is observed for Freundlich model in Table 2. Furthermore, for Freundlich model, the standard deviation with a value of 3.73% is the second smallest among the isotherm models used in this study. Accordingly, the adsorption of bromide on MIEX resin can be well described by the Freundich isotherm model. The Freundlich isotherm model allows for several kinds of adsorption sites on the solid surface and represents properly the adsorption data at low and intermediate concentrations on heterogeneous surfaces [49]. In this study, the bromide concentration ranges from 1–10 mg L^{-1}, being consistent with the assumption of Freundlich model. Furthermore, the MIEX resin is a kind of macro-porous resin, which indicates the surface of MIEX resin is heterogeneous. The photos obtained from Scanning Electron Microscope also show that the surface of MIEX resin is heterogeneous. These are the reasons why the Freundlich model can well describe the adsorption equilibrium data of bromide on MIEX resin. The value of n, one of Freundlich constants, relates to the surface heterogeneity of adsorbent, giving an indication of how favorable an adsorption process. When $0 < 1/n < 1$, the adsorption is favorable; $1/n = 1$, the adsorption is homogeneous and there is no interaction among the adsorbed species; $1/n > 1$, the adsorption is unfavorable [50]. As can be noticed in our study, the value of $1/n$ is 0.55, and ranges from 0 to 1, showing that the adsorption of bromide on MIEX resin is favorable.

Also, it can be seen from Table 2 that the correlation coefficient with a value of 0.9911 for the R–P isotherm model, is very close to

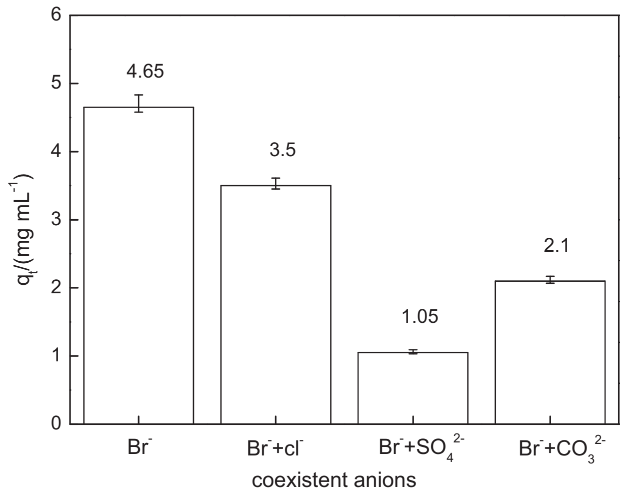

Fig. 6. Effect of coexistent anions on bromide removal (bromide concentration = 5 mg L^{-1}; adsorbent dosage = 1.0 mL L^{-1}; agitation speed = 100 rpm; pH without any adjustment; temperature = 285 K).

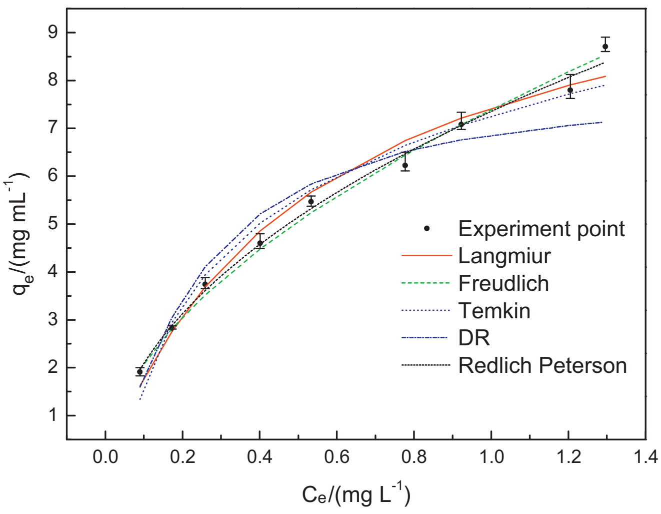

Fig. 7. Adsorption isotherm of bromide on MIEX resin at 303 K.

Table 2
Constants, correlation coefficients and standard deviations of Langmuir, Freundlich, Temkin, D–R and R–P isotherm models.

Model	Constants			R^2	SD (%)
Langmuir	$q_{\max}$ (mg mL^{-1})	b (L mg^{-1})		0.9721	7.16
$\frac{C_e}{q_e} = \frac{C_e}{q_{\max}} + \frac{1}{q_{\max} b}$	11.51	1.82			
Freundlich	k_f	$1/n$		0.9946	3.73
$\log q_e = \frac{1}{n} \log C_e + \log k_f$	7.4	0.55			
Temkin	A (L mg^{-1})	B		0.9659	12.11
$q_e = B \ln C_e + B \ln A$	19.16	2.46			
Dubinin–Radushkevich	$q_{\max}$	B_{DR}		0.9415	11.8
$\ln q_e = -B_{DR}\varepsilon^2 + \ln q_{\max}$	7.75	4×10^{-8}			
Redlich–Peterson	A (L mg^{-1})	B	β	0.9911	3.03
$q_e = \frac{AC_e}{1+BC_e^{\beta}}$	79.83	9.85	0.54		

that of Freundlich isotherm model. In addition, the standard deviation with a value of 3.03% for R–P isotherm model is the smallest among the isotherm models used in this study. Accordingly, the R–P isotherm model can also well describe the equilibrium adsorption of bromide on MIEX resin. For R–P isotherm model, it is a hybrid isotherm featuring both Langmuir and Freundlich isotherms. This may be a reason why the R–P isotherm model gives a good simulation.

The predicted curves by different isotherm models in Fig. 7 also show that both Freundlich and R–P models give satisfactory fits to the equilibrium adsorption data of bromide on MIEX resin, compared to other isotherm models investigated in this study.

3.8. Adsorption kinetics

Adsorption kinetics quantitatively describes the removal efficacy of adsorbate on adsorbent as time elapses. It is crucial for designing the adsorption facilities and understanding the adsorption types and mechanisms. The pseudo first-order and pseudo second-order models are used to fit the kinetics data of bromide adsorption on MIEX resin at different initial bromide concentrations (5, 10 and 20 mg L^{-1}), respectively. The intra-particle diffusion model is further tested to analyze the diffusion mechanism of bromide in adsorption system. These kinetic models can be expressed by Eqs. (10)–(12) [39,51]:

$$\text{Pseudo first-order model}: \ln(q_e - q_t) = \ln q_e - k_1 t \tag{10}$$

$$\text{Pseudo second-order model}: \frac{t}{q_t} = \frac{1}{k_2 q_e^2} + \frac{1}{q_e} t \tag{11}$$

$$\text{Intra-particle diffusion model}: q_t = k_{id} t^{1/2} + C_i \tag{12}$$

where k_1 and k_2 are the rate constants of pseudo first-order and pseudo second-order, respectively. And k_{id} is the intra-particle diffusion rate constant.

The results fitted by pseudo first-order, second-order and intra-particle diffusion models are listed in Table 3. The method of accessing the validity of kinetics models is identical to that of isotherm models.

Table 3 shows that the values (0.9995–0.9996) of correlation coefficients (R^2) for pseudo second-order model are much better than those of the pseudo first-order model, revealing clearly the pseudo second-order model can fit the adsorption of bromide on MIEX resin quite well. It is also observed that compared with the pseudo first-order model, the values (4.20–4.64%) of standard deviations (SD) for pseudo second-order model are much smaller, further indicating that the adsorption process of bromide on MIEX resin can be well described by the pseudo second-order model. In addition, the calculated equilibrium adsorption capacities ($q_{e,\text{cal}}$) obtained from the pseudo second-order model at three initial bromide concentrations of 5, 10 and 20 mg L^{-1} are 4.76, 9.02 and 15.72 mg mL^{-1}, respectively. They are perfectly close to the experimental results ($q_{e,\text{exp}}$). Whereas the calculated values of $q_{e,\text{cal}}$ obtained from the pseudo first-order model are much smaller than the experimental values. This further verifies that the adsorption of bromide on MIEX resin follows the pseudo second-order model well. Accordingly, the adsorption of bromide on MIEX resin is chemical adsorption process involving valence forces through exchange or sharing of electrons between bromide ions and adsorbent [52].

The initial adsorption rate h_0 (mg mL^{-1} min^{-1}) is defined as follows [51]:

$$h_0 = k_2 q_e^2 \tag{13}$$

As shown in Table 3, the initial adsorption rate h_0 obtained from the pseudo second-order model increases from 0.8142 to 4.0032 mg mL^{-1} min with increasing the initial bromide concentration from 5 to 20 mg L^{-1}. This is likely due to the fact that increasing the initial bromide concentration elevates the concentration gradient between the liquid and solid phase, leading to the increase in adsorption driving force [53].

The adsorption process of adsorbate molecules or ions from the bulk liquid phase onto the porous solid adsorbent generally involves three stages: (1) mass transfer of the adsorbate molecules or ions across the external boundary layer (film diffusion); (2) adsorbate molecules or ions diffusion within the pores of the adsorbent (intra-particle diffusion); (3) adsorption or exchange at a site on the surface of adsorbent [54]. In generally, the third step is assumed to be very fast and does not represent the rate limiting step of the whole adsorption process [55]. So the adsorption rate is limited by film diffusion and/or intra-particle diffusion. If the adsorption process of bromide on MIEX resin follows the intra-particle diffusion, the plot of q_t versus $t^{1/2}$ should be linear. Further, the intra-particle diffusion is the only rate limiting process if the plot passes through the origin. It is shown clearly in Fig. 8 that the plots of q_t versus $t^{1/2}$ are not linear over whole time range but multi-linear. Also, the multi-linear plots do not pass through the origin. These results show that the intra-particle diffusion is not the sole rate limiting step in the adsorption process of bromide on MIEX resin, and some other steps along with intra-particle diffusion may be involved in the adsorption process, such as film diffusion [56]. Fig. 8 shows that the plots can be divided into three sections. From 0 min to 5 min, bromide ions are transported to the external surface of adsorbent through the boundary layer diffusion (film diffusion) and the external surface adsorption occurs. As the adsorption continues, the external surface adsorption sites are saturated. Then the adsorption process enters the second stage (from 5 min to 30 min). In this stage, the bromide concentration gradient decreases gradually, and the adsorption of bromide on MIEX resin is controlled by film diffusion and intra-particle diffusion. The final section (from 60 min to 120 min) is the equilibrium adsorption stage where intra-particle diffusion starts to slow down due to the extremely low bromide concentration [38]. It is found in Table 3 that in initial stage, the rate constant, k_{id1}, ranges from 1.0416 to 3.8882 mg mL^{-1} min^{-1} when the initial bromide concentration increases from 5 to 20 mg L^{-1}. This shows the adsorption of bromide

Table 3

The results fitted by pseudo first-order and second-order kinetics models.

C_0 (mg L^{-1})	$q_{e,\exp}$ (mg mL^{-1})	Pseudo first-order model				Pseudo second-order model					Intraparticle diffusion model								
		$q_{e,\mathrm{cal}}$ (mg mL^{-1})	k_1 (mg mL^{-1}· min^{-1})	R^2	SD (%)	$q_{e,\mathrm{cal}}$ (mg mL^{-1})	k_2 (mg mL^{-1} min^{-1})	h_0	R^2	SD (%)	k_{id1} (mg mL^{-1} min$^{-1/2}$)	C_1	R^2	k_{id2} (mg mL^{-1} min$^{-1/2}$)	C_2	R^2	k_{id3} (mg mL^{-1} min$^{-1/2}$)	C_3	R^2
5	4.51	2.56	0.0518	0.9803	58.76	4.76	0.0359	0.8124	0.9995	4.20	1.0416	0	1	0.5347	1.1293	0.9992	0.0239	4.2455	0.9982
10	8.66	3.61	0.0466	0.9439	73.86	9.02	0.0247	2.0068	0.9996	4.32	2.0748	0	1	1.1203	2.1806	0.9916	0.0592	8.0146	0.9925
20	15.18	5.52	0.0448	0.9190	78.94	15.72	0.0162	4.0032	0.9996	4.64	3.0020	0	1	1.8783	4.4817	0.9863	0.1154	13.9360	0.9833

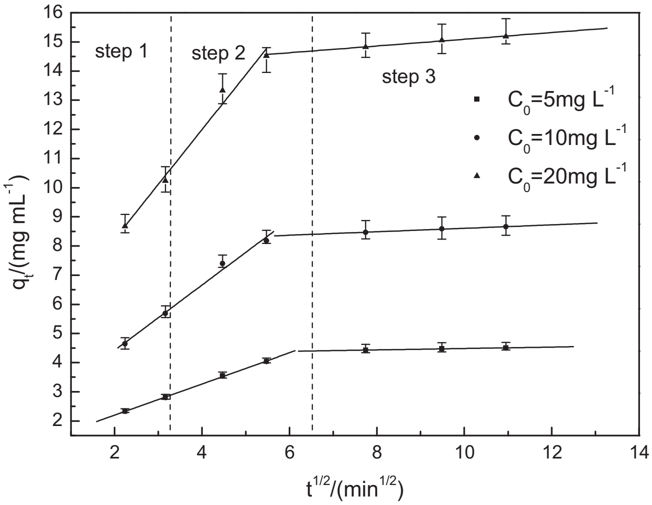

Fig. 8. The intra-particle diffusion model plot for adsorption of bromide on MIEX resin.

on MIEX resin is very fast in initial stage, which may further verify the occurrence of external surface adsorption or film diffusion. However, the rate constants of the second and third stages are much smaller than those of the initial stage, also showing the existence of intra-particle diffusion. Table 3 shows the C_i value of the third stage is much greater than that of the second stage for a constant initial bromide concentration (for example 5 mg L^{-1}). It is also observed from Table 3 that the C_i value increases with increasing the initial bromide concentration from 5 to 20 mg L^{-1}. An increase in C_i value reflects the increase in the thickness of boundary layer, which decreases the change of external mass diffusion and increases the change of internal mass transfer [51]. Hence the intra-particle diffusion may also partly control the adsorption process of bromide on MIEX resin as well as the film diffusion.

3.9. Adsorption thermodynamics

Thermodynamics analysis can provide some detailed information to understand the adsorption process of bromide on MIEX resin from the aspect of energy change. The thermodynamics parameters such as standard enthalpy change (ΔH°, kJ mol^{-1}), standard entropy change (ΔS°, J mol^{-1} K^{-1}) and standard Gibbs free energy change (ΔG°, kJ mol^{-1}), can be calculated by the following equations [39]:

$$\ln K_D = \frac{\Delta S^\circ}{R} - \frac{\Delta H^\circ}{RT} \tag{14}$$

$$\Delta G^\circ = \Delta H^\circ - T\Delta S^\circ \tag{15}$$

where K_D (L mL^{-1}) is the distribution coefficient and calculated by Eq. (3); R (8.314 J mol^{-1} K^{-1}) is universal gas constant.

ΔH° and ΔS° of bromide on MIEX resin can be obtained from the slope and intercept of the plot of $\ln K_D$ against $1/T$ (presented in Fig. 9). Then ΔG° can be calculated by Eq. (15). The thermodynamics parameters calculated are tabulated in Table 4.

The values for standard Gibbs free energy changes are found to be negative at all temperatures investigated in this study, showing that the adsorption of bromide on MIEX resin is thermodynamically feasible and is a spontaneous process. Meanwhile, the ΔG° value becomes less negative with increasing the temperature of solution, indicating that elevating temperature of solution has an adverse effect on the adsorption of bromide on MIEX resin. But the values of ΔG° are close to each other with an increase in temperature of solution from 285 K to 333 K, showing the effect of temperature of solution on bromide removal is slight and such spontaneity is

Table 4
Thermodynamic parameters for bromide adsorption by MIEX resin.

Temperature (K)	K_D (L mL^{-1})	ΔG° (kJ mol^{-1})	ΔH° (kJ mol^{-1})	ΔS° (J mol^{-1} K^{-1})
285	12.16	−5.91	−9.30	−11.89
293	10.63	−5.82		
303	9.87	−5.70		
313	8.62	−5.58		
333	6.81	−5.34		

Table 5
Comparison of bromide sorption capacity using MIEX resin with other adsorbents.

Adsorbent	q_{max}	Conditions					Reference
		C_0 (Br$^-$)	DOC (mg L^{-1})	[Cl$^-$] (mg L^{-1})	Adsorption time	Adsorbent dosage	
A-Ag-15	3.01 μmol g^{-1} ≈ 0.24 mg g^{-1}	0–0.8 mg L^{-1}	0	0			[16]
A-Ag-50	1.58 μmol g^{-1} ≈ 0.13 mg g^{-1}		0	0			[16]
A-Ag-200	0.83 μmol g^{-1} ≈ 0.07 mg g^{-1}		0	0			[16]
A-Ag-15	1.91 μmol g^{-1} ≈ 0.15 mg g^{-1}		0	40			[16]
A-Ag-15	2.44 μmol g^{-1} ≈ 0.20 mg g^{-1}		1.4	4	7 days	0.1 g/100 mL = 1 g L^{-1}	[16]
A-Ag-15	2.04 μmol g^{-1} ≈ 0.16 mg g^{-1}		3.6	3.8			[16]
Activated carbon	0.25 μmol g^{-1} ≈ 0.02 mg g^{-1}		0	0			[16]
MgAl–CO_3 layered double hydroxides	362.3 mg g^{-1}	0–1000 mg L^{-1}	–	–	24 h	0.05 g/50 mL = 1 g L^{-1}	[20]
MIEX resin	11.51 mg mL^{-1}	1–10 mg L^{-1}	–	–	2 h	1 ml L^{-1}	Present study

independent on the temperature [54]. The negative value in standard enthalpy change shows that the heat is released during the adsorption, proving the adsorption of bromide on MIEX resin is an exothermic process. This has been found earlier from Fig. 5. In addition, the negative value in standard entropy change demonstrates the decrease in randomness at the solid/liquid interface after adsorption. This may be attributed to the fact that the affinity of bromide ion to the active adsorption site of MIEX resin is higher than that of chloride ion used as exchange ion, leading to a decrease in disorder of solid/solid interface. Furthermore, the standard entropy change is calculated to be −11.89 J mol^{-1} K^{-1} and is less than −10 J mol^{-1} K^{-1}, implying that the adsorption of bromide on MIEX is an associative mechanism [57].

3.10. *Comparison of bromide adsorption on MIEX resin with other adsorbents*

The adsorption capacity of adsorbent is a significant parameter which can be used to calculate the needed adsorbent dosage in order to obtain a predicted removal efficacy for the given bromide solution. The maximum sorption capacity (q_{max}) obtained from Langmuir model is usually used for the comparison of different sorbents. The adsorption removal of bromide on MIEX resin is compared with those of other adsorbents reported in some literatures [16,20]. The results are presented in Table 5. Although it is difficult to compare MIEX resin with other adsorbents directly because of the maximum adsorption capacities obtained under different experimental conditions, the bromide removal by MIEX resin is effective and the time needed to reach equilibrium is short about 60 min. This may be due to the smaller size of MIEX resin particle, 2–5 times smaller than conventional resin, which increases the specific surface area of MIEX resin sharply and accelerates the adsorption process. The shorter time needed to reach equilibrium for MIEX resin is significant to diminish the size of adsorption facilities. As to the comparison on bromide removal by MIEX resin for different type waters, the results are given in Table 6 (given in online supporting information). The results show that the impurities in waters have significant effect on bromide removal [24,30,36,46,58].

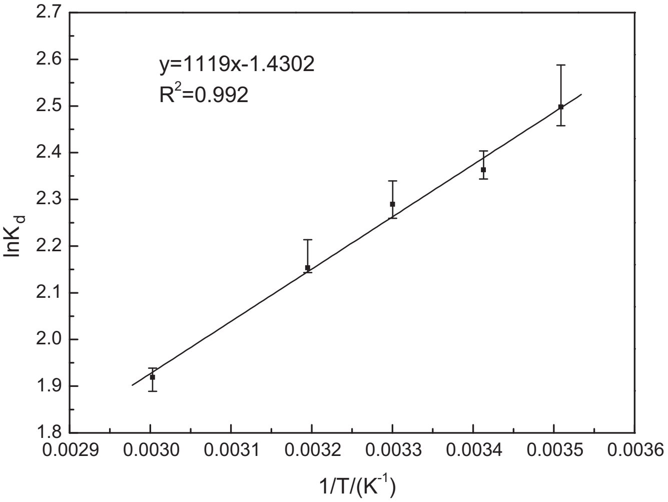

Fig. 9. The plot used to calculate the thermodynamics parameters of bromide adsorption on MIEX resin.

4. Conclusions

The present work shows that MIEX resin can be used as an effective adsorbent for bromide removal from aqueous solutions. The uptake of bromide on MIEX resin increases with increasing the initial bromide concentration. Also, the removal rate of bromide increases with increasing adsorbent dosage. For bromide removal by MIEX resin, the agitation speed of 100 rpm is appropriate. The high removal efficiency of bromide is obtained at the pH range of 4–9. The uptake of bromide decreases with increasing temperature of solution. The coexistent anions have significant effect on bromide removal, and the following sequence is given: $SO_4{}^{2-} > CO_3{}^{2-} > Cl^-$. The equilibrium adsorption of bromide on MIEX resin at 303 K can be well fitted by both Freundich and R–P isotherm models. And the kinetics process of bromide on MIEX resin can be well described by the pseudo second-order model. The diffusion simulation shows the intra-particle diffusion is not the only rate limiting step. The thermodynamics studies show that the adsorption of bromide on MIEX resin is a thermodynamically feasible, spontaneously exothermic process in nature.

Acknowledgements

This work was supported by National Science and Technology Major Project for Water Pollution Control and Treatment of PR China (Grant no. 2008ZX07425-007), Key Natural Science Project for University of Ahui Province (KJ2011Z042) and Research Fund of Anhui University of Technology for Young Teachers (QZ201008).

Appendix A. Supplementary data

Supplementary data associated with this article can be found, in the online version, at doi:10.1016/j.cej.2011.11.096.

References

[1] S.G. Liu, Z.L. Zhu, Y.L. Qiu, J.F. Zhao, Effect of ferric and bromide ions on the formation and speciation of disinfection byproducts during chlorination, J. Environ. Sci. China 23 (2011) 765–772.

[2] CSEPA, China Environmental Aspect (Water Environmental) in 2002, China Environmental Science Press, Beijing, 2003.

[3] K. Listiarini, J.T. Tor, D.D. Sun, J.O. Leckie, Hybrid coagulation–nanofiltration membrane for removal of bromate and humic acid in water, J. Membr. Sci. 365 (2010) 154–159.

[4] H.Y. Zhai, X.R. Zhang, Formation and decomposition of new and unknown polar brominated disinfection byproducts during chlorination, Environ. Sci. Technol. 45 (2011) 2194–2201.

[5] Q.Y. Wu, Y. Li, H.Y. Hu, Y.X. Sun, F.Y. Zhao, Reduced effect of bromide on the genotoxicity in secondary effluent of a municipal wastewater treatment plant during chlorination, Environ. Sci. Technol. 44 (2010) 4924–4929.

[6] W.J. Huang, C.Y. Chang, F.H. Shih, Disinfection by-product formation and mutagenic assay caused by preozonation of groundwater containing bromide, Environ. Monit. Assess. 158 (2009) 181–196.

[7] M. Siddiqui, G. Amy, K. Ozekin, P. Westerhoff, Modeling dissolved ozone and bromate ion formation in ozone contactors, Water Air Soil Pollut. 108 (1998) 1–32.

[8] J.A. Wisniewski, M. Kabsch-Korbutowicz, Bromate removal in the ion-exchange process, Desalination 261 (2010) 197–201.

[9] U. Pinkernell, U. von Gunten, Bromate minimization during ozonation: mechanistic considerations, Environ. Sci. Technol. 35 (2001) 2525–2531.

[10] R. Chitrakar, Y. Makita, A. Sonoda, T. Hirotsu, Fe–Al layered double hydroxides in bromate reduction: synthesis and reactivity, J. Colloid Interface Sci. 354 (2011) 798–803.

[11] X. Huang, N.Y. Gao, Bromate ion formation in dark chlorination and ultraviolet/chlorination processes for bromide-containing water, J. Environ. Sci. 20 (2008) 246–251.

[12] R.J. Garcia-Villanova, M.V.O.D. Leite, J.M.H. Hierro, S.D. Alfageme, C.G. Hernandez, Occurrence of bromate, chlorite and chlorate in drinking waters disinfected with hypochlorite reagents: tracing their origins, Sci. Total Environ. 408 (2010) 2616–2620.

[13] L.A. Ding, Q. Li, H. Cui, R. Tang, H. Xu, X.C. Xie, J.P. Zhai, Electrocatalytic reduction of bromate ion using a polyaniline-modified electrode An efficient and green technology for the removal of BrO_3^- in aqueous solutions, Electrochim. Acta 55 (2010) 8471–8475.

[14] E. Agus, N. Voutchkov, D.L. Sedlak, Disinfection by-products and their potential impact on the quality of water produced by desalination systems: a literature review, Desalination 237 (2009) 214–237.

[15] S. Echigo, S. Itoh, M. Kuwahara, Bromide removal by hydrotalcite-like compounds in a continuous system, Water Sci. Technol. 56 (2007) 117–122.

[16] M. Sanchez-Polo, J. Rivera-Utrilla, E. Salhi, U. von Gunten, Ag-doped carbon aerogels for removing halide ions in water treatment, Water Res. 41 (2007) 1031–1037.

[17] M. Sanchez-Polo, J. Rivera-Utrilla, U. von Gunten, Bromide and iodide removal from waters under dynamic conditions by Ag-doped aerogels, J. Colloid Interface Sci. 306 (2007) 183–186.

[18] F. Ge, H.M. Shu, Y.Z. Dai, Removal of bromide by aluminium chloride coagulant in the presence of humic acid, J. Hazard. Mater. 147 (2007) 457–462.

[19] F. Ge, L.Z. Zhu, Effects of coexisting anions on removal of bromide in. drinking water by coagulation, J. Hazard. Mater. 151 (2008) 676–681.

[20] L.A. Lv, W. Wang, M. Wei, H.J. Cheng, Bromide ion removal from contaminated water by calcined and uncalcined MgAl–CO_3 layered double hydroxides, J. Hazard. Mater. 152 (2008) 1130–1137.

[21] D.E. Kimbrough, I.H. Suffet, Electrochemical removal of bromide and reduction of THM formation potential in drinking water, Water Res. 36 (2002) 4902–4906.

[22] S. Chellam, Effects of nanofiltration on trihalomethane and haloacetic acid precursor removal and speciation in waters containing low concentrations of bromide ion, Environ. Sci. Technol. 34 (2000) 1813–1820.

[23] T.H. Boyer, P.C. Singer, A pilot-scale evaluation of magnetic ion exchange treatment for removal of natural organic material and inorganic anions, Water Res. 40 (2006) 2865–2876.

[24] S. Hsu, P.C. Singer, Removal of bromide and natural organic matter by anion exchange, Water Res. 44 (2010) 2133–2140.

[25] M. Drikas, M. Dixon, J. Morran, Long term case study of MIEX pre-treatment in drinking water; understanding NOM removal, Water Res. 45 (2011) 1539–1548.

[26] P.A. Neale, M. Mastrup, T. Borgmann, A.I. Schafer, Sorption of micropollutant estrone to a water treatment ion exchange resin, J. Environ. Monitor. 12 (2010) 311–317.

[27] I. Kowalska, Anionic surfactant removal by ion exchange, Ochr. Sr. 31 (2009) 25–29.

[28] H.C. Kim, B.A. Dempsey, Removal of organic acids from EfOM using anion exchange resins and consequent reduction of fouling in UF and MF, J. Membr. Sci. 364 (2010) 325–330.

[29] T.H. Boyer, P.C. Singer, G.R. Aiken, Removal of dissolved organic matter by anion exchange: effect of dissolved organic matter properties, Environ. Sci. Technol. 42 (2008) 7431–7437.

[30] T.H. Boyer, P.C. Singer, Bench-scale testing of a magnetic ion exchange resin for removal of disinfection by-product precursors, Water Res. 39 (2005) 1265–1276.

[31] I. Kowalska, Ion-exchange-ultrafiltration system for surfactants removal from water solutions, Desalination Water Treat. 25 (2011) 47–53.

[32] C. Liu, W. Chen, Z. Cao, J.L. Li, R. van Merkenstein, Removal of algogenic organic matter by MIEX (R) pre-treatment and its effect on fouling in ultrafiltration, Fresenius Environ. Bull. 19 (2010) 3118–3124.

[33] T. Bond, E.H. Goslan, S.A. Parsons, B. Jefferson, Disinfection by-product formation of natural organic matter surrogates and treatment by coagulation, MIEX (R) and nanofiltration, Water Res. 44 (2010) 1645–1653.

[34] M. Drikas, M. Dixon, J. Morran, Removal of MIB and geosmin using granular activated carbon with and without MIEX pre-treatment, Water Res. 43 (2009) 5151–5159.

[35] H. Humbert, H. Gallard, H. Suty, J.P. Croue, Natural organic matter (NOM) and pesticides removal using a combination of ion exchange resin and powdered activated carbon (PAC), Water Res. 42 (2008) 1635–1643.

[36] H. Humbert, H. Gallard, H. Suty, J.P. Croue, Performance of selected anion exchange resins for the treatment of a high DOC content surface water, Water Res. 39 (2005) 1699–1708.

[37] AQSIQ, Methods for Examination of Drinking Natural Mineral Water, China Standards Press, Beijing, 2009.

[38] K.S. Tong, M.J. Kassim, A. Azraa, Adsorption of copper ion from its aqueous solution by a novel biosorbent *Uncaria gambir*: equilibrium, kinetics, and thermodynamic studies, Chem. Eng. J. 170 (2011) 145–153.

[39] L. Ding, H.P. Deng, X. Han, L. Dong, P. Wang, D. de Ridder, Adsorption characteristics of phosphate from aqueous solutions by sponge iron: isotherm, kinetics, and thermodynamics studies, Fresenius Environ. Bull. 19 (2010) 2548–2561.

[40] X.P. Liao, B. Shi, Adsorption of fluoride on zirconium(IV)-impregnated collagen fiber, Environ. Sci. Technol. 39 (2005) 4628–4632.

[41] A.A.M. Daifullah, S.M. Yakout, S.A. Elreefy, Adsorption of fluoride in aqueous solutions using $KMnO_4$-modified activated carbon derived from steam pyrolysis of rice straw, J. Hazard. Mater. 147 (2007) 633–643.

[42] A.K. Golder, A.N. Samanta, S. Ray, Removal of phosphate from aqueous solutions using calcined metal hydroxides sludge waste generated from electrocoagulation, Sep. Purif. Technol. 52 (2006) 102–109.

[43] G.L. Xiao, Y.G. Fan, P.L. Helian, Z.Q. Shi, Study on preparation and thermostability of two types strongly basin anion exchange resins, Ion Exchange Adsorpt 21 (2005) 514–531.

[44] L.M. Blaney, S. Cinar, A.K. SenGupta, Hybrid anion exchanger for trace phosphate removal from water and wastewater, Water Res. 41 (2007) 1603–1613.

[45] F. Deniz, S. Karaman, Removal of Basic Red 46 dye from aqueous solution by pine tree leaves, Chem. Eng. J. 170 (2011) 67–74.

[46] P.C. Singer, K. Bilyk, Enhanced coagulation using a magnetic ion exchange resin, Water Res. 36 (2002) 4009–4022.

[47] K.Y. Foo, B.H. Hameed, Insights into the modeling of adsorption isotherm systems, Chem. Eng. J. 156 (2010) 2–10.

[48] E. Bulut, M. Özacar, İ.A. Şengil, Equilibrium and kinetic data and process design for adsorption of Congo red onto bentonite, J. Hazard. Mater. 154 (2008) 613–622.

[49] D.L. Zhao, G.D. Sheng, J. Hu, C.L. Chen, X.K. Wang, The adsorption of Pb(II) on Mg_2Al layered double hydroxide, Chem. Eng. J. 171 (2011) 167–174.

[50] M.A. Rauf, S.B. Bukallah, F.A. Hamour, A.S. Nasir, Adsorption of dyes from aqueous solutions onto sand and their kinetic behavior, Chem. Eng. J. 137 (2008) 238–243.

[51] X.L. Han, W. Wang, X.J. Ma, Adsorption characteristics of methylene blue onto low cost biomass material lotus leaf, Chem. Eng. J. 171 (2011) 1–8.

[52] M. Al-Ghouti, M.A.M. Khraisheh, M.N.M. Ahmad, S. Allen, Thermodynamic behaviour and the effect of temperature on the removal of dyes from aqueous solution using modified diatomite: a kinetic study, J. Colloid Interface Sci. 287 (2005) 6–13.

[53] B. Noroozi, G.A. Sorial, H. Bahrami, M. Arami, Equilibrium and kinetic adsorption study of a cationic dye by a natural adsorbent – silkworm pupa, J. Hazard. Mater. 139 (2007) 167–174.

[54] R.I. Yousef, B. El-Eswed, A.H. Al-Muhtaseb, Adsorption characteristics of natural zeolites as solid adsorbents for phenol removal from aqueous solutions:

kinetics, mechanism, and thermodynamics studies, Chem. Eng. J. 171 (2011) 1143–1149.
[55] C.M. Sun, G.H. Zhang, R.J. Qu, Y. Yu, Removal of transition metal ions from aqueous solution by crosslinked polystyrene-supported bis-8-oxyquinoline-terminated open-chain crown ethers, Chem. Eng. J. 170 (2011) 250–257.
[56] A.B. Albadarin, A.H. Al-Muhtaseb, N.A. Al-laqtah, G.M. Walker, S.J. Allen, M.N.M. Ahmad, Biosorption of toxic chromium from aqueous phase by lignin: mechanism, effect of other metal ions and salts, Chem. Eng. J. 169 (2011) 20–30.
[57] K. Gobi, M.D. Mashitah, V.M. Vadivelu, Adsorptive removal of Methylene Blue using novel adsorbent from palm oil mill effluent waste activated sludge: equilibrium, thermodynamics and kinetic studies, Chem. Eng. J. 171 (2011) 1246–1252.
[58] C.J. Johnson, P.C. Singer, Impact of a magnetic ion exchange resin on ozone demand and bromate formation during drinking water treatment, Water Res. 38 (2004) 3738–3750.